biology letters

Apparent density patterns in subchondral bone of the sloth and anteater forelimb

Biren A Patel and Kristian J Carlson

Biol. Lett. 2008 **4**, 486-489
doi: 10.1098/rsbl.2008.0297

biology letters

Biol. Lett. (2008) **4**, 486–489
doi:10.1098/rsbl.2008.0297
Published online 15 July 2008

Biomechanics

Apparent density patterns in subchondral bone of the sloth and anteater forelimb

Biren A. Patel[1,*] **and Kristian J. Carlson**[2]

[1]*Department of Biomedical Sciences, Ohio University College of Osteopathic Medicine, Athens, OH 45701, USA*
[2]*Department of Anatomy, New York College of Osteopathic Medicine, Old Westbury, NY 11568, USA*
**Author for correspondence (patelb@oucom.ohiou.edu).*

Vertebrate morphologists often are interested in inferring limb-loading patterns in animals characterized by different locomotor repertoires. Because bone apparent density (i.e. mass per unit volume of bone inclusive of porosities) is a determinant of compressive strength, and thus indicative of compressive loading, recent comparative studies in primates have proposed a structure–function relationship between apparent density of subchondral bone and locomotor behaviours that vary in compressive loading. If such patterns are found in other mammals, then these relationships would be strengthened further. Here, we examine the distal radius of suspensory sloths that generally load their forelimbs (FLs) in tension and of quadrupedal anteaters that generally load their FLs in compression. Computed tomography osteoabsorptiometry was used to visualize the patterns in subchondral apparent density. Suspensory sloths exhibit relatively smaller areas of high apparent density than quadrupedal anteaters. This locomotor-based pattern is analogous to the pattern observed in suspensory and quadrupedal primates. Similarity between xenarthran and primate trends suggests broad-scale applicability for analysing subchondral bone apparent density and supports the idea that bone functionally alters its material properties in response to locomotor behaviours.

Keywords: functional morphology; quadrupedal; radius; suspensory; wrist

1. INTRODUCTION

Apparent density of bone is a primary determinant of its compressive strength both through the amount of mineral (i.e. tissue density) and the degree of porosity exhibited by the bone (Currey 1984; Keller 1994). Compressive strength of subchondral bone is particularly revealing of habitual compressive loading in a limb because it serves as the site of force transmission across diarthrodial joints (Radin *et al.* 1970). When joint surfaces are relatively congruent (i.e. predominantly experience compressive loading rather than bending), apparent density can be visualized to estimate habitual loading regimes (Müller-Gerbl *et al.* 1992; Eckstein *et al.* 1999). Although extrapolating behavioural differences from comparisons of bone material properties is not without its share of complexities, these properties still provide valuable insights for biologists interested in structure–function interactions (e.g. Demes *et al.* 2001; Lieberman *et al.* 2003; Pearson & Lieberman 2004; Ruff *et al.* 2006).

Compressive loading of a joint is predominantly a function of (i) joint reaction forces arising from muscle–tendon complexes crossing the joint and (ii) gravitational forces operating on body mass that is supported through the joint (i.e. body weight). A recent 'natural experiment' comparing primates that experience compressive forelimb (FL) loads falling into both categories (i.e. quadrupeds) versus primates restricted to the former category (i.e. suspensory and bipedal) suggested that body weight may take priority in establishing subchondral apparent density (Carlson & Patel 2006). Radiodensity of subchondral bone at the distal radial articular surface differed between these two primate locomotor groups. Old World monkeys (Cercopithecoids) and African apes (*Pan* and *Gorilla*) had relatively broader areas of high apparent density compared with suspensory Asian apes (*Hylobates* and *Pongo*) and bipedal humans (Carlson & Patel 2006). Asian apes habitually restrict compressive forces generated through their wrist to those arising from muscle contractions (i.e. joint reaction forces) since they suspend their body mass below superstrata (and increase tension through their FL; Swartz *et al.* 1989). In addition, as Biewener (1989) has shown for terrestrial mammals, suspensory support may reduce muscle force requirements, and thus compressive bone loading, owing to alignment of the FL and its joints with superstratum reaction forces associated with suspensory support. Humans do not support body weight through their FLs during locomotion and thus they too will habitually limit compressive forces across the wrist joint to muscle contractile forces. Since monkeys and African apes, unlike the other primate groups, typically are required to support body mass above substrates during quadrupedalism, Carlson & Patel (2006) suggested that their more expansive areas of high apparent density corresponded to superimposed compressive loads in the wrist joint due to muscle contractile forces and body weight support. Others have noted additional links between locomotor behaviour and bone material properties in the primate postcranial skeleton (e.g. Schaffler & Burr 1984; DeRousseau 1988).

If the relationship between subchondral apparent density patterns and habitual locomotor modes can be extended beyond primates, it may indicate the presence of a broad-scale trend among vertebrates. It also would bolster the argument that bone modulates its properties according to functional input (e.g. locomotor behaviour). Here, we investigate xenarthrans as an independent test of a previously identified primate trend. Others have demonstrated functional and morphological convergences between extant xenarthrans and some non-human primates (Mendel 1979; Orr 2005). We also selected xenarthrans because they are phylogenetically distant from primates (Springer *et al.* 2004) and exhibit behavioural diversity (e.g. quadrupedal and suspensory species; Nowak 1999). Specifically, we compare suspensory sloths (*Bradypus* and *Choloepus*), which

Received 1 June 2008
Accepted 24 June 2008

probably habitually load FLs in tension, to quadrupedal anteaters (*Myrmecophaga* and *Tamandua*), which probably habitually load FLs in compression.

2. MATERIAL AND METHODS

Distal radii were examined in 33 sloths (*Choloepus didactylus*, *Choloepus hoffmanni*, *Bradypus tridactylus* and *Bradypus variegatus*) and anteaters (*Myrmecophaga tridactyla*, *Tamandua mexicana*, *Tamandua tetradactyla*). We selected only wild-shot specimens with epiphyseal plate fusion of all long bones (skeletally adult), no/minimal signs of degenerative joint disease or traumatic injury and no post-mortem abrasion to the distal radius (Carlson & Patel 2006).

Computed tomography osteoabsorptiometry was used to visualize apparent density (i.e. radiodensity) of subchondral bone at the distal radius (Müller-Gerbl *et al.* 1992; Carlson & Patel 2006). Radii were serially CT scanned (GE lightspeed 16; slice thickness, 0.625 mm; tube voltage, 120 kV; tube current, 70 mA) in parasagittal planes. Elements were scanned individually to maximize the accuracy of grey values for each specimen. Reconstruction of raw CT data used a soft tissue algorithm. Reconstructed digital images were saved as DICOM files and imported into ImageJ software (http://rsb.info.nih.gov/ij) for subsequent evaluation. From each image stack, two-dimensional maximum intensity projection (MIP) maps were generated by visualizing brightness values of the three-dimensional data volume (see Carlson & Patel 2006). Brightness values of pixels in the MIP were partitioned into eight distinct colour bins by creating a false colour map. The lowest bin (white) included pixels with minimal radiodensities, while the highest bin (black) contained pixels with maximal radiodensities (figure 1*a*). Pixels in each bin were counted and calculated as a percentage of the total pixels in the articular surface, although we emphasize only the maximum bin (i.e. black pixels) during comparisons within and between locomotor groups. By using percentages of total articular surface area, we accounted for size effects (body size). Group differences were evaluated using non-parametric Mann–Whitney *U*-tests.

3. RESULTS AND DISCUSSION

The amount of maximal apparent density in the articular surface of the distal radius is greater in xenarthrans that habitually load their FLs in compression (i.e. quadrupedalism) compared with those that reduce compression in their FLs (i.e. increase tension by adopting more suspensory postures). Quadrupedal anteaters (*Myrmecophaga* and *Tamandua*) have expanded areas of high apparent density (i.e. greater black pixels relative to total pixels in the articular surface) compared with suspensory sloths (*Choloepus* and *Bradypus*; figure 1 and table 1; $U=10$; $p<0.001$). Significant differences, however, do not extend to taxa within locomotor groups (figure 1*b*). The quadrupedal anteaters—the giant *Myrmecophaga* and the smaller *Tamandua*—do not differ from one another in the relative areas of high apparent density ($U=33$; $p=0.694$), nor do the suspensory sloths—the two-toed *Choloepus* and the three-toed *Bradypus* ($U=8$; $p=0.079$). Considering that both groups probably have strong digital flexor muscles for either digging (anteaters) or hanging below superstrata (sloths), the added weight support by quadrupedal anteaters could be a probable explanation for their increased area of maximal apparent density.

It is intriguing that xenarthrans in both locomotor groups exhibit relatively more expansive high apparent density areas than those reported in the respective suspensory and quadrupedal primates (i.e. 6.0% and 16.2% of articular surface area in the suspensory and quadrupedal primates, respectively; table 1; Carlson & Patel 2006). Because compressive loading

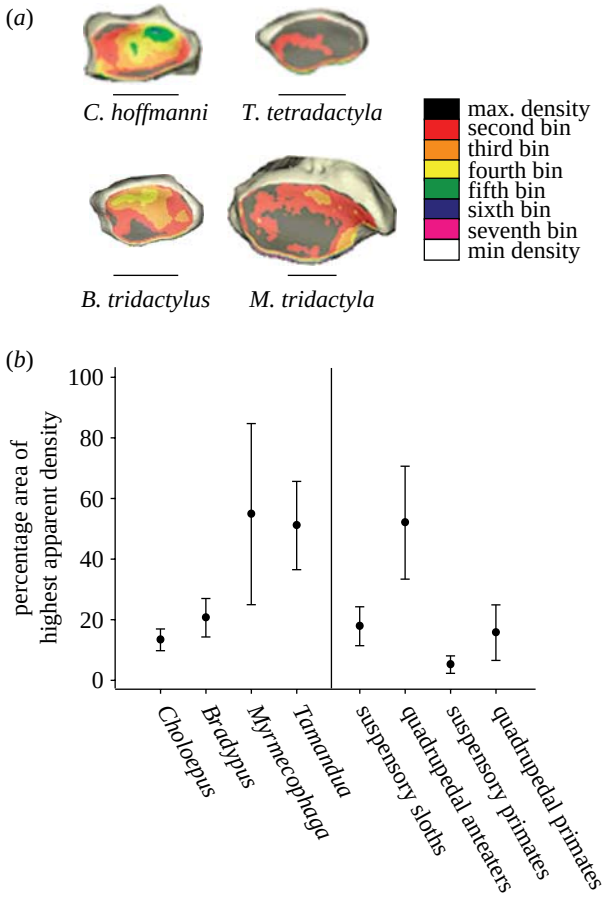

Figure 1. (*a*) Representative MIPs for each xenarthran genus. Scale bar, 1 cm. (*b*) Percentage area of highest apparent density for each xenarthran genus and each locomotor group (suspensory and quadrupedal xenarthrans and primates). Primate data adapted from Carlson & Patel (2006). Boxes, means; whiskers, 1 s.d.

should impact apparent density of subchondral bone, potential differences in locomotor kinetics between xenarthrans and primates may be relevant. Primates generally experience lower peak vertical substrate reaction forces (SRFs) in their FLs relative to their hind limbs (HL) than most other mammals during linear quadrupedal locomotion on runways and simulated arboreal substrates (Demes *et al.* 1994). The relatively unique primate interlimb SRF pattern could be related to a more posterior location of the centre of mass in primates, or to a dynamic caudal shift of the body weight towards the HL during primate locomotion (Reynolds 1985). While SRF data from xenarthrans have not been published, trends in interlimb SRFs among non-primate mammals appear robust (Demes *et al.* 1994). If xenarthrans were found to support a greater proportion of their body weight on their FLs, much like non-primate mammals in general, FL/HL kinetic distinctions from primates would be consistent with non-primates exhibiting relatively greater amounts of high apparent density in their wrist joint. There are caveats, however, to such a scenario. Behavioural variability of free-ranging animals is probably more dynamic than often modelled in the laboratory, and thus the overall variability in SRFs for any one phylogenetic group (e.g. primates and xenarthrans)

Table 1. Percentage areas (% pixels) of apparent density in MIPs[a].

	mass (kg)[b]		% max	% second	% third	% fourth	% fifth
Choloepus	6.25	mean	13.4	30.1	28.2	13.8	4.7
$n=5$		s.d.	3.6	15.3	7.9	9.1	3.5
Bradypus	4.25	mean	20.7	36.1	24.3	6.9	2.5
$n=8$		s.d.	6.3	7.9	7.9	3.7	0.5
Myrmecophaga	28.5	mean	54.8	24.1	9.9	3.4	1.6
$n=5$		s.d.	29.9	16.9	14.0	4.5	1.0
Tamandua	4.5	mean	51.1	24.9	6.0	3.5	3.0
$n=15$		s.d.	14.6	10.1	2.4	1.3	1.1
suspensory sloths		mean	17.8	33.8	25.8	9.5	3.4
$n=13$		s.d.	6.4	11.1	7.8	6.9	2.3
quadrupedal anteaters		mean	52.0	24.7	7.0	3.5	2.6
$n=20$		s.d.	18.6	11.6	7.0	2.3	1.2
suspensory primates[c]		mean	6.0	17.9	30.2	25.7	9.9
$n=12$		s.d.	2.9	7.2	8.0	7.7	8.6
quadrupedal primates[c]		mean	16.2	23.3	27.3	19.8	5.3
$n=33$		s.d.	8.2	10.7	7.4	11.7	4.1

[a] Percentages calculated as the number of pixels in a colour bin divided by the total number of pixels in the articular surface. Colour scale in figure 1*a* provides bin definitions.
[b] Genus means from Nowak (1999).
[c] Data adapted from Carlson & Patel (2006).

remains poorly understood. Additionally, differences in high apparent density areas between xenarthrans and primates could also be a phylogenetic effect (i.e. genetic difference).

Despite the relatively greater areas of high apparent density in xenarthrans relative to primates, it is important to note the parallel between suspensory versus quadrupedal xenarthrans and between suspensory and quadrupedal primates (Carlson & Patel 2006). Similarities between the locomotor groups that cross phylogenetic boundaries suggest a robust structure–function signal. Functional morphologists could use patterns in apparent density of subchondral bone to evaluate habitual joint loading when experimental data are untenable. A widely applicable signal also supports the notion that bone modulates its material properties, at least partially according to behavioural activities (e.g. locomotor behaviour). Therefore, studies of subchondral bone (Ahluwalia 2000; Carlson & Patel 2006; Patel & Carlson 2007; Polk *et al.* 2008) augments the expanding breadth of research into cortical and trabecular bone structure by functional morphologists (e.g. Lieberman *et al.* 2003; Pearson & Lieberman 2004; Pontzer *et al.* 2006; Ruff *et al.* 2006).

No live animals were used in this study and all data were obtained from museum specimens.

We thank the American Museum of Natural History (Eileen Westwig), National Museum of Natural History (Linda Gordon) and Museum of Comparative Zoology (Judy Chupasko) for access to specimens. CT scanning was facilitated by Stony Brook University Hospital with help from Lou Caronia, Justin Georgia and Andrew Farke.

Ahluwalia, K. 2000 Knee joint load as determined by tibial subchondral bone density: its relationship to gross morphology and locomotor behavior in catarrhines. PhD dissertation, Stony Brook University.

Biewener, A. A. 1989 Scaling body support in mammals: limb posture and muscle mechanics. *Science* **245**, 45–48. (doi:10.1126/science.2740914)

Carlson, K. J. & Patel, B. A. 2006 Habitual use of the primate forelimb is reflected in the material properties of subchondral bone in the distal radius. *J. Anat.* **208**, 659–670. (doi:10.1111/j.1469-7580.2006.00555.x)

Currey, J. D. 1984 Comparative mechanical properties of histology of bone. *Am. Zool.* **24**, 5–12.

Demes, B., Larson, S. G., Stern Jr, J. T., Jungers, W. L., Biknevicius, A. R. & Schmitt, D. 1994 The kinetics of primate quadrupedalism—hindlimb drive reconsidered. *J. Hum. Evol.* **26**, 353–374. (doi:10.1006/jhev.1994.1023)

Demes, B., Qin, Y.-X., Stern Jr, J. T., Larson, S. G. & Rubin, C. T. 2001 Patterns of strain in the macaque tibia during functional activity. *Am. J. Phys. Anthropol.* **116**, 257–265. (doi:10.1002/ajpa.1122)

DeRousseau, C. J. 1988 Osteoarthritis in rhesus monkeys and gibbons: a locomotor model of joint degeneration. *Contrib. Primatol.* **25**, 1–145.

Eckstein, F., Merz, B., Schön, M., Jacobs, C. R. & Putz, R. 1999 Tension and bending, but not compression alone determine the functional adaptation of subchondral bone in incongruous joints. *Anat. Embryol.* **199**, 85–97. (doi:10.1007/s004290050212)

Keller, T. S. 1994 Predicting the compressive mechanical behavior of bone. *J. Biomech.* **27**, 1159–1168. (doi:10.1016/0021-9290(94)90056-6)

Lieberman, D. E., Pearson, O. M., Polk, J. D., Demes, B. & Crompton, A. W. 2003 Optimization of bone growth and remodeling in response to loading in tapered mammalian limbs. *J. Exp. Biol.* **206**, 2135–3138. (doi:10.1242/jeb.00514)

Mendel, F. C. 1979 The wrist joint of two-toed sloths and its relevance to brachiating adaptations in the Hominoidea. *J. Morphol.* **162**, 413–424. (doi:10.1002/jmor.1051620308)

Müller-Gerbl, M., Putz, R. & Kenn, R. 1992 Demonstration of subchondral bone density patterns by three-dimensional CT osteoabsorptiometry as a non-invasive method for *in vivo* assessment of individual long-term stresses in joints. *J. Bone Miner. Res.* **7**, S411–S418.

Nowak, R. M. 1999 *Walker's mammals of the world*, 6th edn. Baltimore, MD: The Johns Hopkins University Press.

Orr, C. M. 2005 Knuckle-walking anteater: a convergence test of adaptation for purported knuckle-walking features of African Hominidae. *Am. J. Phys. Anthropol.* **128**, 639–658. (doi:10.1002/ajpa.20192)

Patel, B. A. & Carlson, K. J. 2007 Bone density spatial patterns in the distal radius reflect habitual hand postures adopted by quadrupedal primates. *J. Hum. Evol.* **52**, 130–141. (doi:10.1016/j.jhevol.2006.08.007)

Pearson, O. M. & Lieberman, D. E. 2004 The aging of Wolff's 'law': ontogeny and responses to mechanical loading in cortical bone. *Yrbk Phys. Anthropol.* **47**, 63–99. (doi:10.1002/ajpa.20155)

Polk, J. D., Blumenfeld, J. & Ahluwalia, K. 2008 Knee posture predicted from subchondral apparent density in the distal femur: an experimental validation. *Anat. Rec.* **291**, 293–302. (doi:10.1002/ar.20653)

Pontzer, H., Lieberman, D. E., Momin, E., Devlin, M. J., Polk, J. D., Hallgrimsson, B. & Cooper, D. M. L. 2006 Trabecular bone in the bird knee responds to high sensitivity to changes in load orientation. *J. Exp. Biol.* **209**, 57–65. (doi:10.1242/jeb.01971)

Radin, E. L., Paul, I. L. & Lowy, M. 1970 A comparison of the dynamic force transmitting properties of subchondral bone and articular cartilage. *J. Bone Joint Surg.* **52A**, 444–456.

Reynolds, T. R. 1985 Mechanics of increased support of weight by the hindlimbs in primates. *Am. J. Phys. Anthropol.* **67**, 335–349. (doi:10.1002/ajpa.1330670406)

Ruff, C., Holt, B. & Trinkaus, E. 2006 Who's afraid of the big bad Wolff? 'Wolff's law' and bone functional adaptation. *Am. J. Phys. Anthropol.* **129**, 484–498. (doi:10.1002/ajpa.20371)

Schaffler, M. B. & Burr, D. B. 1984 Primate cortical bone microstructure: relationship to locomotion. *Am. J. Phys. Anthropol.* **65**, 191–197. (doi:10.1002/ajpa.1330650211)

Springer, M. S., Stanhope, M. J., Madsen, O. & de Jong, W. W. 2004 Molecules consolidate the placental mammal tree. *Trends Ecol. Evol.* **19**, 430–438. (doi:10.1016/j.tree.2004.05.006)

Swartz, S. M., Bertram, J. E. A. & Biewener, A. A. 1989 Telemetered *in vivo* strain analysis of locomotor mechanics of brachiating gibbons. *Nature* **342**, 270–272. (doi:10.1038/342270a0)